Published in final edited form as:
Clin Chim Acta. 2013 May ; 420: 62–68. doi:10.1016/j.cca.2013.03.016.

Proteomic Analysis of Postsynaptic Density in Alzheimer Disease

Jianying Zhou, **Drew R. Jones**, **Duc M. Duong**, **Allan I. Levey**, **James J Lah**, and **Junmin Peng**
St. Jude Children's Research Hospital, 262 Danny Thomas Pl., Memphis, TN 38105-3678, 901-336-1083, junmin.peng@stjude.org

Abstract

Background—The loss of synaptic function is a pivotal mechanism in the development of Alzheimer's Disease (AD). Structural changes and loss of plasticity in the postsynaptic density (PSD) may contribute to the pathogenesis. However, the underlying molecular events triggering synaptic dysfunction remain elusive. We report a quantitative proteomics analysis of the PSD from human postmortem brain tissues of possible and definite AD cases.

Method—The analysis used both discovery and targeted mass spectrometry approaches and was repeated with biological replicates. During the discovery study, we compared several hundred proteins in the PSD-enriched fractions and found that 25 proteins were differentially regulated in AD.

Results—Interestingly, the majority of these protein changes were larger in definite AD cases than in possible AD cases. In the targeted analysis, we measured the level of 9 core PSD proteins and found that only IRSp53 was highly down-regulated in AD. The alteration of selected proteins (i.e. internexin and IRSp53) was further validated by immunoblotting against 7 control and 8 AD cases.

Conclusions—These results expand our understanding of how AD impacts PSD composition, and hints at new hypotheses for AD pathogenesis.

Keywords

Alzheimer; Disease; Proteomics; Mass spectrometry; Synapse

1. Introduction

Alzheimer's Disease (AD) progresses over time, ultimately causing death after robbing patients of basic cognitive functions and placing a large burden on the health-care system. Although the exact etiology of the disease remains poorly understood, the amyloid and tau hypotheses [1,2], which have largely driven the field for the preceding two decades, have significantly advanced our understanding of the mechanisms of cognitive decline. Although amyloid plaques and neurofibrillary tangles represent the neuropathological features most closely identified with AD, changes in the number and function of synapses are correlated better with cognitive symptoms than either plaques or tangles [3,4]. It is now believed that

soluble oligomers of Aβ play a key role in triggering synaptic defects in AD [5]. Morphological alteration of postsynaptic structures and functional change of synaptic signaling may contribute to AD. The molecular details, however, are not fully elucidated.

The postsynaptic density (PSD) is an essential structure for excitatory signaling and plasticity in mammalian neurons [6,7]. The PSD includes numerous neurotransmitter receptors, scaffold proteins, cytoskeleton components and other regulatory elements, which are assembled together to form a highly compact proteinaceous disk-like structure, approximately 30–40 nm thick and a few hundred nm wide [8]. The neurotransmitter receptors in the PSD are organized into supramolecular complexes that are biochemically compact and are resistant to extraction of mild detergents (e.g. Triton X-100), which renders the method for its purification. These organized protein networks provide an efficient assembly for signal transduction and are regulated to allow strengthening and weakening of synaptic transmission. Moreover, protein constituents of the PSD are known to be dynamically influenced by synaptic activity, via mechanisms such as local translation, protein phosphorylation, ubiquitination, and degradation, as well as protein translocation into and out of synapses [9,10].

Continuing proteomic studies have revealed the complexity of the PSD, with approximately 1,000 core proteins being identified [11–14]. Additionally, these proteins are rich and diverse in regulatory modifications such as phosphorylation [15–18] and ubiquitination [19–22]. Much effort suggests that specific PSD components are impacted in AD, but an understanding of the proteome-wide changes in the PSD associated with AD remains lacking. Because of the cardinal role of the PSD in synaptic regulation, proteomics study of the PSD is important for understanding the AD pathogenesis.

We sought to determine the impact of AD progression on the PSD constituents through clinical proteomic analysis of post-mortem tissues. These tissue samples enabled age-matched studies to be carried out, in both possible AD and definite AD, with the benefit of having well-characterized clinical pathology and demographic information. We utilized a previously optimized PSD purification protocol [12] to isolate the PSD using sucrose gradient centrifugation followed by mild detergent extraction. The isolated PSD samples were analyzed by discovery proteomics and targeted mass spectrometric methods, revealing novel proteins that may be involved in synaptic dysregulation during the AD progression.

2. Materials and methods

2.1. Post-mortem Sample Information

Human post-mortem tissues from cortical area (Table S1) were provided from clinically and pathologically well characterized cases at the Alzheimer's Disease Research Center (ADRC), Center for Neurodegenerative Disease (CND) Brain Bank at Emory University School of Medicine. Diagnoses were made in accordance with established criteria and guidelines of control and AD [23,24]. Namely, tissues were assessed for neuritic plaques with a qualitative score of none, moderate, or frequent assigned to each sample. Similarly, neurofibriliary tangles were assessed and Braak scores were assigned on a scale of 1–6. Finally, a CERAD (Consortium to Establish a Registry for Alzheimer's Disease) diagnosis was assigned, indicating possible Alzheimer's Disease, or definite Alzheimer's Disease.

2.2. Preparation of Postsynaptic Density from Clinical Tissue

PSD fractions were prepared from post-mortem brain cortex similar to previously described methods [12,13] (Fig. 1A). Brain tissue (~1 g) was homogenized on ice in Buffer A (5 mmol/l 4-(2-hydroxyethyl)-1-piperazineethanesulfonic acid (HEPES), pH 7.4, 1 mmol/l $MgCl_2$, 0.5 mmol/l $CaCl_2$, 0.1 mmol/l phenylmethylsulfonyl fluoride) with Teflon

homogenizer (12 strokes). Brain homogenate was centrifuged at 1,400 × *g* for 10 min to generate supernatant 1 (S1) and pellet 1 (P1). The S1 was further centrifuged at 13,800 × *g* for 10 min to collect supernatant 2 (S2) and the crude synaptosomal pellet (P2). The P2 was resuspended in Buffer B (0.32 mol/l sucrose, 6 mmol/l Tris, pH 8.0, 0.1 mmol/l phenylmethanesulfonylfluoride protease inhibitor) by Teflon homogenizer (5 strokes), loaded onto a discontinuous sucrose gradient (0.85 M/1 M/1.2 mol/l in 6 mmol/l Tris, pH 8.0), and centrifuged at 82,500 × *g* (OptimaTM Ultracentrifuge, Sw 41 Ti rotor) for 2 h. The synaptosomal fraction between 1 and 1.2 mol/l sucrose (P3) was collected and adjusted to 1 ml with Buffer B. Equal volume of Buffer C (6 mmol/l Tris, pH 8.1, and 1% Triton X-100) was added, mixed for 15 min and centrifuged at 32,800 × g for 20 min to obtain the PSD pellet. PSD proteins were dissolved in Buffer D (50 mmol/l Tris, pH 8.5 and 1.0% SDS) at 95°C for 5 min. The protein concentration was determined by BIO-RAD protein assay using BSA as standard, and was further confirmed by silver staining of samples loaded on a short SDS gel [25]. PSD enrichment factor was estimated as ~ 8.5 by western blot method using antibodies of synaptic protein markers.

2.3. Analysis of the PSD by liquid chromatography-mass spectrometry (LC-MS/MS)

Equal amounts of the PSD samples were resolved on a short 9% SDS gel (~5 mm) and stained with Coomassie Brilliant Blue G-250 followed by destaining to remove salt and detergent. The proteins in every short gel lane were excised into one fraction and subjected to ingel tryptic digestion (1:20 trypsin/substrate ratio) [26]. The resulting peptides were analyzed according to the optimized LC-MS/MS conditions [25] in a 3.5 h gradient elution on an LTQ-Orbitrap mass spectrometer (Thermo Scientific).

MS/MS spectra were searched against a human reference database from the National Center for Biotechnology Information using the SEQUEST Sorcerer algorithm (version 2.0, SAGE-N) [27]. Searching parameters included mass tolerance of precursor ions (± 50 ppm) and product ion (± 0.5 Da), partial tryptic restriction, fixed mass shift for modification of carboxyamidomethylated Cys (+ 57.0215 Da), dynamic mass shifts for oxidized Met (+ 15.9949 Da), three maximal modification sites and three maximal missed cleavages. Only b and y ions were considered during the database match. To evaluate false discovery rate during the spectrum-peptide matching, all original protein sequences were reversed to generate a decoy database that was concatenated to the original database [28,29]. To remove false positive matches, assigned peptides were grouped by charge state and then filtered by minimal peptide length (7 amino acid), mass-to-charge accuracy (± 5 ppm) and matching scores (XCorr and deltaCn) to reduce protein FDR below 1%. If peptides were shared by multiple members of a protein family, the matched members were clustered into a single group. Based on the principle of parsimony, the group was represented by the protein with the highest number of assigned peptides, and by other proteins if they were matched by unique peptide(s), resulting in the acceptance of 492 proteins (Table S2).

2.4. Extracted ion current (EIC) based label-free protein quantification

Label free quantification was carried out using an in-house developed program, DQUAN (Direct Quantification), which extracted the EIC signals of all peptides across multiple runs to calculate peptide ratios. The program first extracted and defined peak information for all sequenced peptides, and selected the strongest peaks for each peptide in every run. To align peptides across different runs, a reference run was selected to compare with all other runs, according to retention time (RT) and mass-to-charge ratio (*m/z*). The drift (i.e., mean and variance) of RT and *m/z* were locally defined based on the same peptides identified in different runs. If one peptide was not identified in some runs, the corresponding peak was defined by matched RT and *m/z*. Matched peptide ratios were then summarized into protein ratios. Outlier peptide ratios were removed by Dixon's Q test [30].

2.5. Quantification of Selected Proteins by the LC-SRM Strategy

The analysis of 9 proteins of interest was analyzed as reported [13]. Synthetic heavy-isotope-labeled peptides (0.2 pmol each except 2 pmol of CaMKIIα and CaMKIIβ) were implemented during in-gel digestion of the PSD samples (~20 μg). The peptide mixtures were then analyzed by LC-SRM twice by loading 10% of the samples with known parameters (Table S3). The quantitative analysis was carried out using Xcalibur software (Thermo Scientific, San Jose, CA).

2.6. Antibodies in Western Blot Analyses

Antibodies used in this study included PSD-95 (Sigma, St. Louis, MO), GluR2 (a gift from Dr. Morgan Sheng, Genentech, South San Francisco, CA), Aβ (4G8, Sigma), internexin (Millipore, Billerica, MA), β-tubulin (Developmental Studies Hybridoma Bank at the University of Iowa), synaptophysin (BD transduction Laboratories), and IRSP53 (Millipore).

3. Results

3.1. Preparation of the PSD from control and AD cases

To study the proteomic change in the PSD of AD brain (Fig. 1A), we set up two experimental sample groups (Table S1). Each group consisted of three age-matched samples of a control, a possible AD case (pAD), and a definite AD case (AD), according to CERAD standardized diagnosis [23]. Prior to the analysis, we probed the Aβ peptide level in the total tissue lysate of all six samples (Fig. 1B). Both cases of definite AD showed strong Aβ formation while control and possible AD replicates showed no detectable Aβ signal, consistent with pathological diagnosis. The samples were then subjected to PSD enrichment using an standard protocol [12] (Fig. 1A). To assess the efficacy of the protocol, we analyzed all fractions by comparative immunoblotting (Fig. 1C). Postsynaptic markers (i.e. PSD-95 and the AMPA (2-amino-3-(3-hydroxy-5-methyl-isoxazol-4-yl)propanoic acid) receptor GluR2 subunit) were increasingly enriched with each step, whereas a presynaptic marker (i.e. synaptophsyin) was largely depleted by Triton X-100 extraction. Tubulin was co-purified in all fractions at almost equal efficiency as previously reported [12]. The PSD proteins from control, pAD, and AD samples were further evaluated by sodium dodecyl sulfate polyacrylamide gel electrophoresis followed by silver staining (Fig. 1D). The overall profiles were largely identical between control and AD samples, showing no significant problem in protein degradation or contamination (e.g. by blood). Moreover, the relative enrichment factor of the PSD fraction was assessed by PSD-95 blot against a titration curve for each sample (Fig. 1E). Across the samples, PSD-95 was enriched by ~9 fold and the enrichment factor was reasonably consistent during sample preparation. Overall, these detailed sample characterization steps demonstrate that it is feasible to enrich the PSD proteins from postmortem brains for quantitative mass spectrometry studies.

3.2. Analysis of the PSD by a discovery proteomics approach

We then performed the label-free quantitative LC-MS/MS of the six PSD samples based on extracted ion currents (Fig. 2A). To minimize the experimental variants, we used a short SDS gel to remove salt and detergent (e.g. SDS) and digested all proteins from each sample in a single gel band. The technical reproducibility of the LC-MS/MS platform was examined by performing technical replicates of a PSD fraction from pAD1. The retention times of identified peptides were recorded, adjusted by peak alignment, and then plotted against each other (Fig. 2B), demonstrating high reproducibility of the LC elution profile and our method. Instrument mass accuracy was also assessed by plotting a histogram of matched peptide mass error in ppm (Fig. 2C). An overall standard deviation of 2.6 ppm showed the

high mass accuracy of the method. Furthermore, to evaluate inter-sample difference, the ratio of peptide intensity between samples was converted into a $\log_2$ ratio to generate the histograms (Fig. 2D). As expected, the technical replicate of pAD1 injections showed the lowest variance with standard deviation (SD) of 0.22. The biological replicate of pAD samples (i.e. pAD1 versus pAD2) showed an increased variance (SD of 0.30), reflecting biological variance in two human samples summed with experimental variance. Finally, the comparison between a control and a definite AD case showed the highest difference (SD of 0.37), indicating extra diseased-related differences in the two samples. From the entire PSD dataset, 1,556 peptides and 494 groups of proteins were identified and compared (Table S2).

Proteins differentially regulated in AD versus control postsynaptic densities were identified by the $\log_2$ ratio of their respective extracted ion currents. Spectral ratio data was recorded for each biological duplicate, and the $\log_2$ values were averaged. We accepted proteins that showed at least 2 fold change (almost three times the standard deviation, ~99% confidence interval), resulting in 25 proteins that demonstrated significant up- or down-regulation in AD postsynaptic density preparations of post-mortem clinical tissues (Table 1). Regulated proteins were categorized according to subcellular location or biological function. The most up-regulated PSD proteins from AD tissue included chaperones, signal transduction proteins, and core metabolic enzymes, while the most down-regulated proteins had mostly mitochondrial origins. The averaged $\log_2$ ratios of the 25 regulated proteins were plotted for control, possible AD, and definite AD cases (Fig. 3). The line graph shows two distinct populations; down-regulated and up-regulated proteins, with proteins for possible AD showing intermediate levels between control and definite AD cases. This important finding suggests that the most of the 25 regulated proteins in this study could correlate with the pathological diagnosis of Alzheimer's Disease.

3.3. Analysis of the PSD by a targeted proteomics approach

As the discovery LC-MS/MS analysis did not include multi-dimensional separation of proteins or peptides, some regulatory PSD components of low abundance may not be detected. Therefore, we used another targeted proteomics method [13] to probe some previously known PSD proteins that were missed in the discovery analysis and also re-quantified some key constitutes with better accuracy. The targeted method involved isotopically heavy standard peptides labeled at valine, leucine, or proline residues (Table S3). The standard peptides were spiked into the in-gel digest, and all peptides were harvested together (Fig. 4A). During the LC elution, the native and labeled peptides were coeluted and analyzed by mass spectrometry in a mode of selected reaction monitoring (SRM), in which the mass-to-charge of the precursor and product ions were pre-defined to avoid the "undersampling" issue in shotgun LC-MS/MS, and thus achieved better sensitivity and reproducibility. Using this LC-SRM strategy, we obtained reliable data for 9 PSD proteins in duplication, and the absolute levels of targeted proteins were reported in picomole, based on known levels of standard (heavy) peptides (Fig. 4B). While most of the PSD proteins showed no significant change, insulin receptor tyrosine kinase substrate of 53 kDa (IRSp53), and Septin7 showed strong decreasing and increasing trends respectively. Compared to control, definite AD cases showed a reduction of approximately two-fold in the IRSp53 level.

3.4. Validation of selected protein changes in AD

To further validate the results of proteomics studies, we collected more control and AD cases for Western blot analysis (Table S1). Individual tissue specimens were homogenized and probed for IRSp53, Internexin, and GluR2 (Fig. 5). Ponceau S (PS) staining also demonstrated the integrity in the proteome and served as a loading control. GluR2 levels showed no change with respect to AD status, in agreement with other null observations of

glutamate receptors in AD [31]. IRSp53 showed significantly decreased levels in AD blots compared to controls, supporting the LC-SRM findings. Internexin was also found to have higher levels across the definite AD cases, consistent with previous reports of internexin as an end-stage marker of AD and structural damage to neurons [32].

4. Discussion

Our study demonstrates the feasibility of isolating the PSD from postmortem brain specimens for quantitative proteomics analysis. Once experimental variations were rigorously monitored, it was practical to perform label-free quantitative analysis of disease tissues. It is worth noting that biological replicates are essential for data analysis and the reduction of false positive discoveries.

Our purpose was to focus on the analysis of PSD protein changes in AD, and biochemical purification led to ~9 fold enrichment of core PSD components. The purification process, however, could not avoid contamination by other subcellular structures that may not be relevant to postsynaptic structure. For instance, a number of metabolic enzymes were identified, suggesting contamination by housekeeping proteins. Mitochondria were also known to be copurified with the PSD [12]. Therefore, we did not validate these proteins during our follow-up analysis. But this does not indicate that these proteins are unimportant or nonfunctional in synapse or in AD development. Indeed, dendritic mitochondria have been reported to contribute to neuron morphogenesis and synaptic plasticity [33], and dysfunction of mitochondria may play a role in AD pathogenesis [34].

Our proteomics findings support other reports in the literature [32] and also uniquely identify a number of novel proteins altered in AD. Significantly, IRSp53 was found to be moderately and strongly down-regulated in possible AD and definite AD cases, respectively. IRSp53 is one of a family of proteins harboring IRSp53–MIM domain that is associated with both actin and lipids [35]. The family of proteins regulate actin dynamics, membrane trafficking and the formation of cellular protrusions. In neurons, IRSp53 has been reported to interact with PSD scaffold proteins (e.g. PSD-95 and chapsyn-110/PSD-93) and function in the small GTPase Rac1/Cdc42 pathway, which regulates actin-based dendritic morphogenesis [36]. Moreover, IRSp53 knockout mice display a decreased size of the PSD and cognitive deficits [37]. Thus, the loss of IRSp53 during the AD progression may be important for mediating the cognitive defects in the disease.

Supplementary Material

Refer to Web version on PubMed Central for supplementary material.

Acknowledgments

This work was partially supported by NIH grants R21AG039764, P30NS055077, and P50AG005136. JP is also supported by ALSAC (American Lebanese Syrian Associated Charities)

References

1. Hardy J, Selkoe DJ. The amyloid hypothesis of Alzheimer's disease: progress and problems on the road to therapeutics. Science. 2002; 297:353–356. [PubMed: 12130773]
2. Ballatore C, Lee VM, Trojanowski JQ. Tau-mediated neurodegeneration in Alzheimer's disease and related disorders. Nat Rev Neurosci. 2007; 8:663–672. [PubMed: 17684513]
3. Terry RD, Masliah E, Salmon DP, et al. Physical basis of cognitive alterations in Alzheimer's disease: synapse loss is the major correlate of cognitive impairment. Ann Neurol. 1991; 30:572–580. [PubMed: 1789684]

4. Selkoe DJ. Alzheimer's disease is a synaptic failure. Science. 2002; 298:789–791. [PubMed: 12399581]
5. Sheng M, Sabatini BL, Sudhof TC. Synapses and Alzheimer's disease. Cold Spring Harbor perspectives in biology. 2012; 4
6. Kennedy MB. Signal-processing machines at the postsynaptic density. Science. 2000; 290:750–754. [PubMed: 11052931]
7. Sheng M, Hoogenraad CC. The Postsynaptic Architecture of Excitatory Synapses: A More Quantitative View. Annu Rev Biochem. 2007; 76:823–847. [PubMed: 17243894]
8. Sheng M. Molecular organization of the postsynaptic specialization. Proc Natl Acad Sci U S A. 2001; 98:7058–7061. [PubMed: 11416187]
9. Ehlers MD. Activity level controls postsynaptic composition and signaling via the ubiquitin-proteasome system. Nat Neurosci. 2003; 6:231–242. [PubMed: 12577062]
10. Trinidad JC, Thalhammer A, Burlingame AL, Schoepfer R. Activity-dependent protein dynamics define interconnected cores of co-regulated postsynaptic proteins. Mol Cell Proteomics. 2012
11. Li KW, Hornshaw MP, Van Der Schors RC, et al. Proteomics analysis of rat brain postsynaptic density. Implications of the diverse protein functional groups for the integration of synaptic physiology. J Biol Chem. 2004; 279:987–1002. [PubMed: 14532281]
12. Peng J, Kim MJ, Cheng D, Duong DM, Gygi SP, Sheng M. Semiquantitative proteomic analysis of rat forebrain postsynaptic density fractions by mass spectrometry. J Biol Chem. 2004; 279:21003–21011. [PubMed: 15020595]
13. Cheng D, Hoogenraad CC, Rush J, et al. Relative and absolute quantification of postsynaptic density proteome isolated from rat forebrain and cerebellum. Mol Cell Proteomics. 2006; 5:1158–1170. [PubMed: 16507876]
14. Collins MO, Husi H, Yu L, et al. Molecular characterization and comparison of the components and multiprotein complexes in the postsynaptic proteome. J Neurochem. 2006; 97(Suppl 1):16–23. [PubMed: 16635246]
15. Collins MO, Yu L, Campuzano I, Grant SG, Choudhary JS. Phosphoproteomic analysis of the mouse brain cytosol reveals a predominance of protein phosphorylation in regions of intrinsic sequence disorder. Mol Cell Proteomics. 2008; 7:1331–1348. [PubMed: 18388127]
16. Munton RP, Tweedie-Cullen R, Livingstone-Zatchej M, et al. Qualitative and quantitative analyses of protein phosphorylation in naive and stimulated mouse synaptosomal preparations. Mol Cell Proteomics. 2007; 6:283–293. [PubMed: 17114649]
17. Trinidad JC, Thalhammer A, Specht CG, et al. Quantitative analysis of synaptic phosphorylation and protein expression. Mol Cell Proteomics. 2008; 7:684–696. [PubMed: 18056256]
18. Edbauer D, Cheng D, Batterton MN, et al. Identification and characterization of neuronal MAP kinase substrates using a specific phosphomotif antibody. Mol Cell Proteomics. 2009; 8:681–695. [PubMed: 19054758]
19. Na CH, Jones DR, Yang Y, Wang X, Xu Y, Peng J. Synaptic Protein Ubiquitination in Rat Brain Revealed by Antibody-based Ubiquitome Analysis. J Proteome Res. 2012 Aug 15. 2012; [Epub ahead of print].
20. Jin Y, Garner CC. Molecular mechanisms of presynaptic differentiation. Annu Rev Cell Dev Biol. 2008; 24:237–262. [PubMed: 18588488]
21. Shen K, Scheiffele P. Genetics and cell biology of building specific synaptic connectivity. Annual review of neuroscience. 2010; 33:473–507.
22. Bingol B, Sheng M. Deconstruction for reconstruction: the role of proteolysis in neural plasticity and disease. Neuron. 2011; 69:22–32. [PubMed: 21220096]
23. Mirra SS, Heyman A, McKeel D, et al. The Consortium to Establish a Registry for Alzheimer's Disease (CERAD). Part II. Standardization of the neuropathologic assessment of Alzheimer's disease. Neurology. 1991; 41:479–486. [PubMed: 2011243]
24. Hyman BT, Trojanowski JQ. Consensus recommendations for the postmortem diagnosis of Alzheimer disease from the National Institute on Aging and the Reagan Institute Working Group on diagnostic criteria for the neuropathological assessment of Alzheimer disease. J Neuropathol Exp Neurol. 1997; 56:1095–1097. [PubMed: 9329452]

25. Xu P, Duong DM, Peng J. Systematical optimization of reverse-phase chromatography for shotgun proteomics. J Proteome Res. 2009; 8:3944–3950. [PubMed: 19566079]
26. Shevchenko A, Wilm M, Vorm O, Mann M. Mass spectrometric sequencing of proteins silver-stained polyacrylamide gels. Anal Chem. 1996; 68:850–858. [PubMed: 8779443]
27. Eng J, McCormack AL, Yates JR 3rd. An approach to correlate tandem mass spectral data of peptides with amino acid sequences in a protein database. J Am Soc Mass Spectrom. 1994; 5:976–989.
28. Peng J, Elias JE, Thoreen CC, Licklider LJ, Gygi SP. Evaluation of multidimensional chromatography coupled with tandem mass spectrometry (LC/LC-MS/MS) for large-scale protein analysis: the yeast proteome. J Proteome Res. 2003; 2:43–50. [PubMed: 12643542]
29. Elias JE, Gygi SP. Target-decoy search strategy for increased confidence in large-scale protein identifications by mass spectrometry. Nat Methods. 2007; 4:207–214. [PubMed: 17327847]
30. Rorabacher DB. Statistical Treatment for Rejection of Deviant Values: Critical Values of Dixon Q Parameter and Related Subrange Ratios at the 95 percent Confidence Level. Anal Chem. 1991; 63:139–146.
31. Gong Y, Lippa CF, Zhu J, Lin Q, Rosso AL. Disruption of glutamate receptors at Shank-postsynaptic platform in Alzheimer's disease. Brain Res. 2009; 1292:191–198. [PubMed: 19635471]
32. Dickson TC, Chuckowree JA, Chuah MI, West AK, Vickers JC. alpha-Internexin immunoreactivity reflects variable neuronal vulnerability in Alzheimer's disease and supports the role of the beta-amyloid plaques in inducing neuronal injury. Neurobiol Dis. 2005; 18:286–295. [PubMed: 15686957]
33. Li Z, Okamoto K, Hayashi Y, Sheng M. The importance of dendritic mitochondria in the morphogenesis and plasticity of spines and synapses. Cell. 2004; 119:873–887. [PubMed: 15607982]
34. Lin MT, Beal MF. Mitochondrial dysfunction and oxidative stress in neurodegenerative diseases. Nature. 2006; 443:787–795. [PubMed: 17051205]
35. Scita G, Confalonieri S, Lappalainen P, Suetsugu S. IRSp53: crossing the road of membrane and actin dynamics in the formation of membrane protrusions. Trends Cell Biol. 2008; 18:52–60. [PubMed: 18215522]
36. Choi J, Ko J, Racz B, et al. Regulation of dendritic spine morphogenesis by insulin receptor substrate 53, a downstream effector of Rac1 and Cdc42 small GTPases. The Journal of neuroscience : the official journal of the Society for Neuroscience. 2005; 25:869–879. [PubMed: 15673667]
37. Sawallisch C, Berhorster K, Disanza A, et al. The insulin receptor substrate of 53 kDa (IRSp53) limits hippocampal synaptic plasticity. J Biol Chem. 2009; 284:9225–9236. [PubMed: 19208628]

Highlights

1. Report a pilot proteomics analysis of synaptic proteins from Alzheimer's disease.
2. Demonstrate the feasibility of isolating postsynaptic density from AD brain.
3. Analyze clinical samples in biological replicates by two proteomics methods.
4. Validate selected proteins (internexin and IRSp53) by immunoblotting.

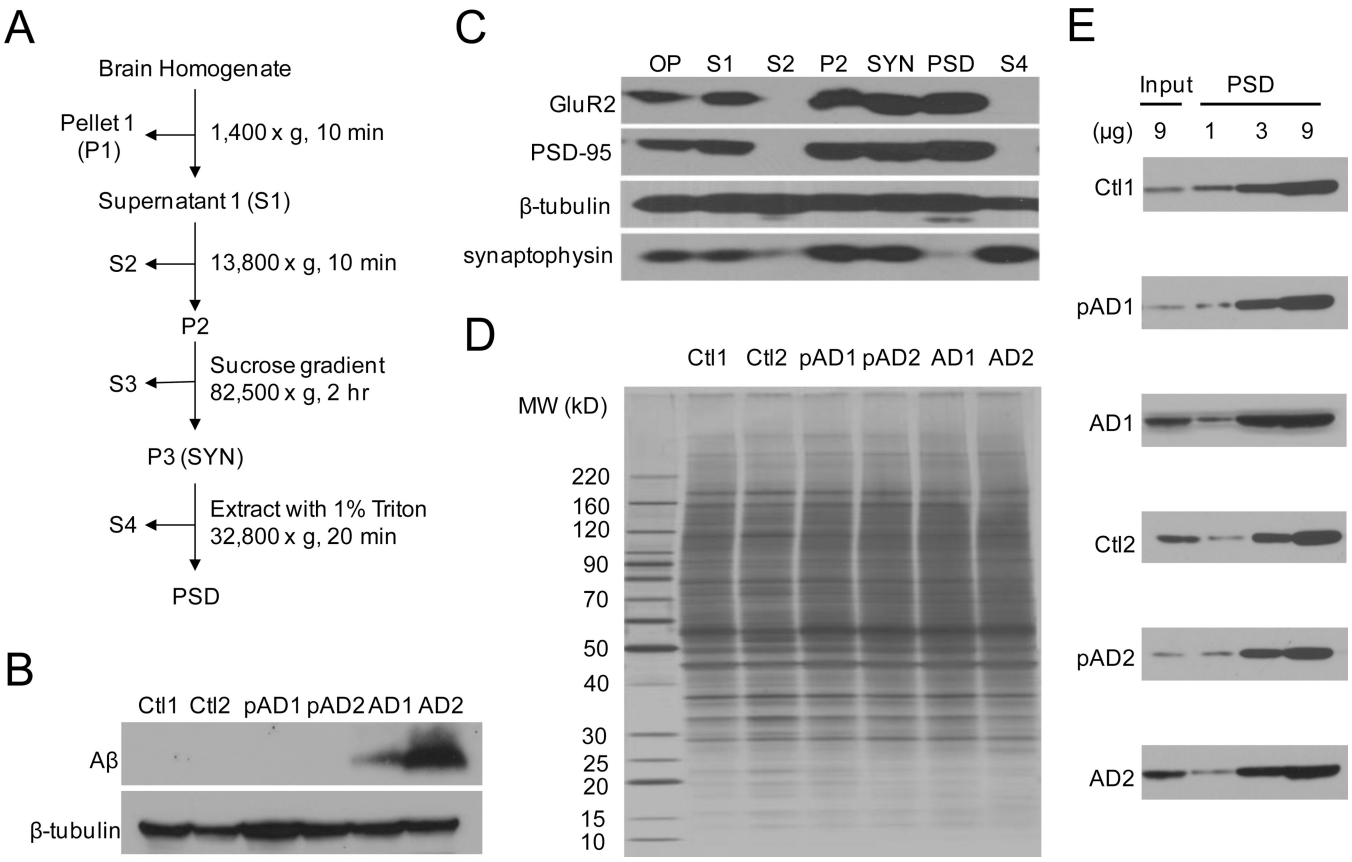

Figure 1. Preparation and validation of postsynaptic density

(**A**) Scheme for enrichment of postsynaptic density from clinical post-mortem tissue samples via differential detergent solubility centrifugation. (**B**) Western blot against amyloid beta (Aβ) peptide in representative cases of control (Ctl), possible Alzheimer's Disease (pAD), and Alzheimer's Disease (AD). (**C**) Validation of post-synaptic density purification by western blot against relevant pre- and post-synaptic protein markers. OP: total brain lysate as onput. The other fractions were shown in panel A. Equal amount of proteins were loaded for every fraction. (**D**) Total protein in PSD fractions of clinical tissue samples assessed by SDS-PAGE. (**E**) Titration and relative enrichment of post-synaptic density material via PSD-95 western blot across control and pathological tissue samples.

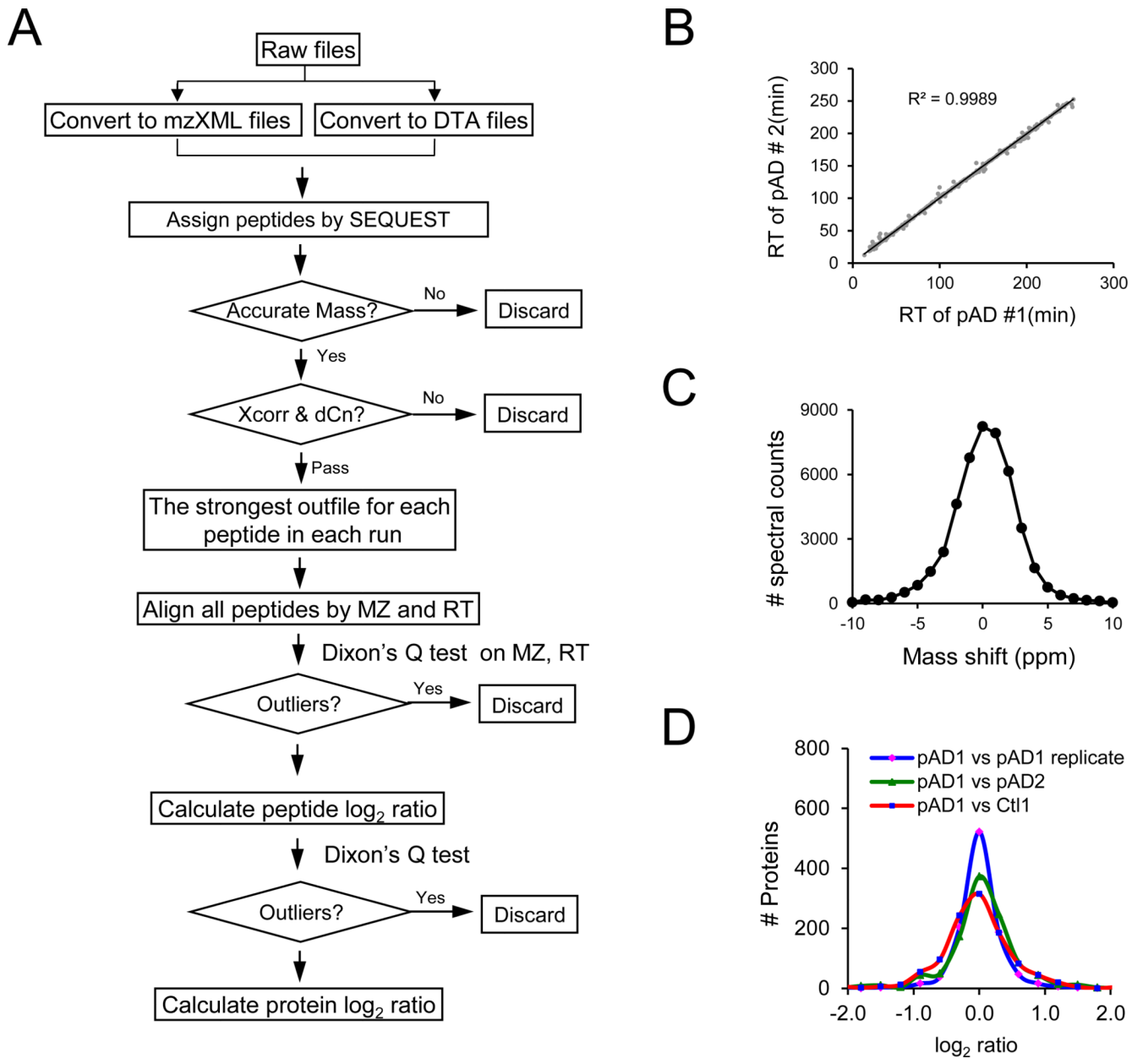

Figure 2. Data analysis workflow and method reproducibility

(**A**) Proteomics data analysis workflow for identification and quantification of proteins (see the METHODS section for details). (**B**) Technical LC-MS/MS injection replicates demonstrating highly reproducible chromatographic elution profiles. (**C**) Global analysis of peptide mass deviation using highresolution Orbitrap MS. The matched MS/MS spectral counts were used before removing redundancy. (**D**) Histogram plot of protein spectral count ratio between AD technical replicates (blue), AD biological replicates (green), and AD vs. control (red). The chart was based on the summarized protein dataset prior to grouping and removing redundancy.

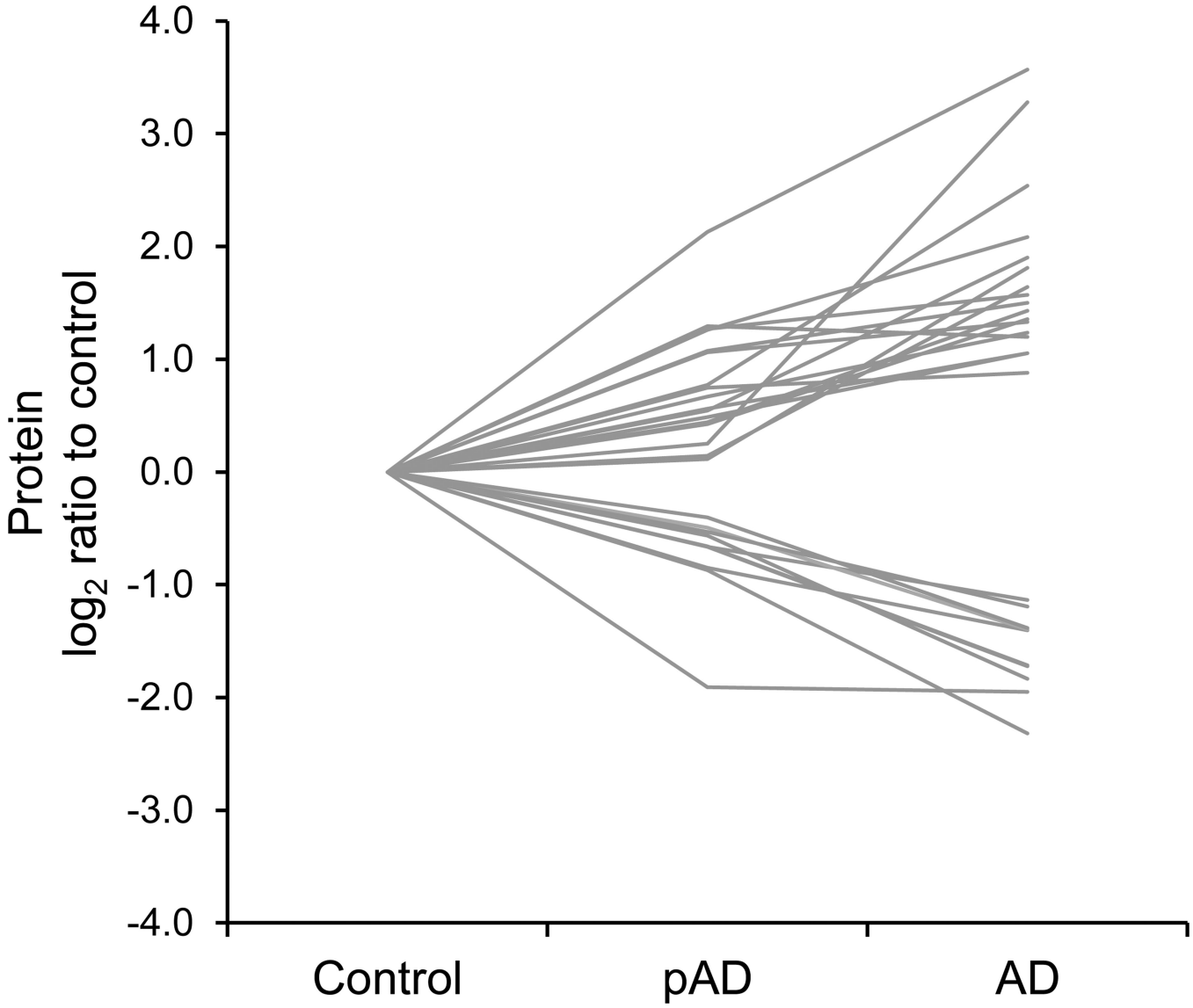

Figure 3. Differential regulation of the identified proteins

Protein abundance ratio to control in possible Alzheimer's Disease cases (pAD) and definite Alzheimer's Disease cases (AD) tissues. Line graph visualizes positive and negative trends across control, intermediate, and pathological phenotypes.

A

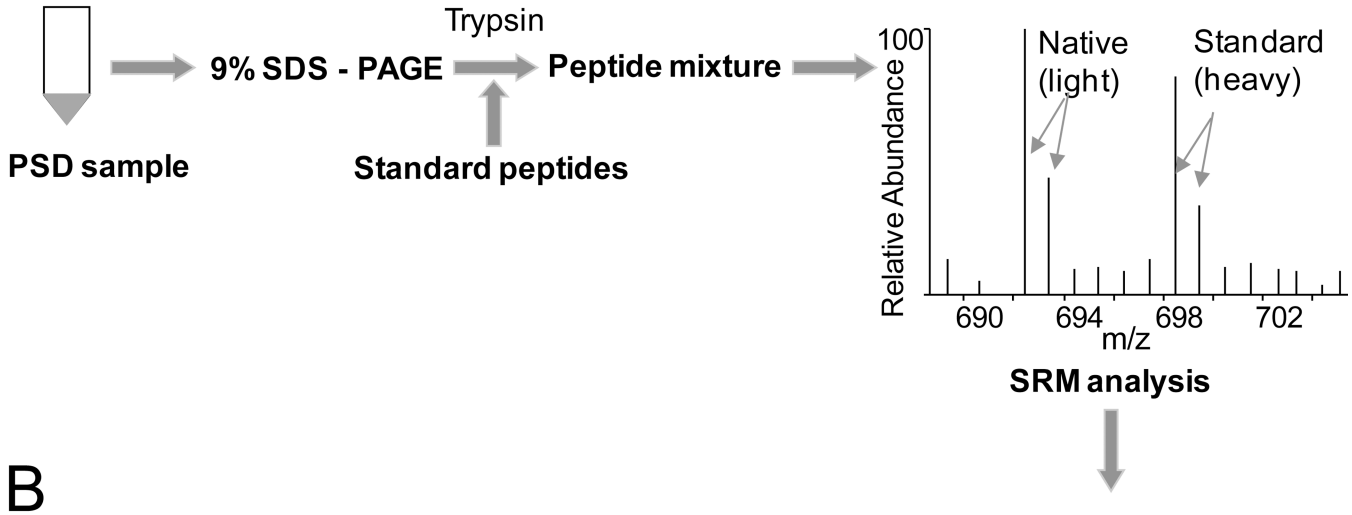

B

Protein Names	Peptide Sequences	pmol		
		Ctl	pAD	AD
IRSp53	GYFDALVK	0.22 ± 0.04	0.16 ± 0.02	0.10 ± 0.02
CaMKIIα	ITQYLDAGGIPR	9.80 ± 0.40	7.80 ± 3.40	8.40 ± 1.00
CaMKIIβ	FTDEYQLYEDIGK	2.80 ± 0.80	2.40 ± 0.60	1.80 ± 0.00
N-cadherin	GPFPQELVR	0.20 ± 0.00	0.18 ± 0.06	0.16 ± 0.00
catenin beta	SGGIPALVK	0.26 ± 0.04	0.26 ± 0.06	0.24 ± 0.02
PSD95	NTYDVVYLK	0.16 ± 0.12	0.18 ± 0.06	0.14 ± 0.02
SAPAP 1/GKAP	SLDSLDPAGLLTSPK	0.40 ± 0.08	0.22 ± 0.04	0.30 ± 0.08
septin7	VNIIPLIAK	5.12 ± 0.82	6.46 ± 6.56	8.04 ± 6.32
SynGAP	AGYVGLVTVPVATLAGR	0.78 ± 0.78	1.54 ± 0.08	0.56 ± 0.38

Figure 4. Quantification of selected post-synaptic density proteins by LC-SRM

(**A**) Workflow for LC-SRM strategy in analysis of proteins from PSD fractions of clinical brain tissue of age-matched control, possible AD, and definite AD cases. Major PSD proteins were targeted based on previously reported peptides. (**B**) Absolute levels of light (endogenous) proteins are reported in pmol based on known levels of heavy (standard) peptides.

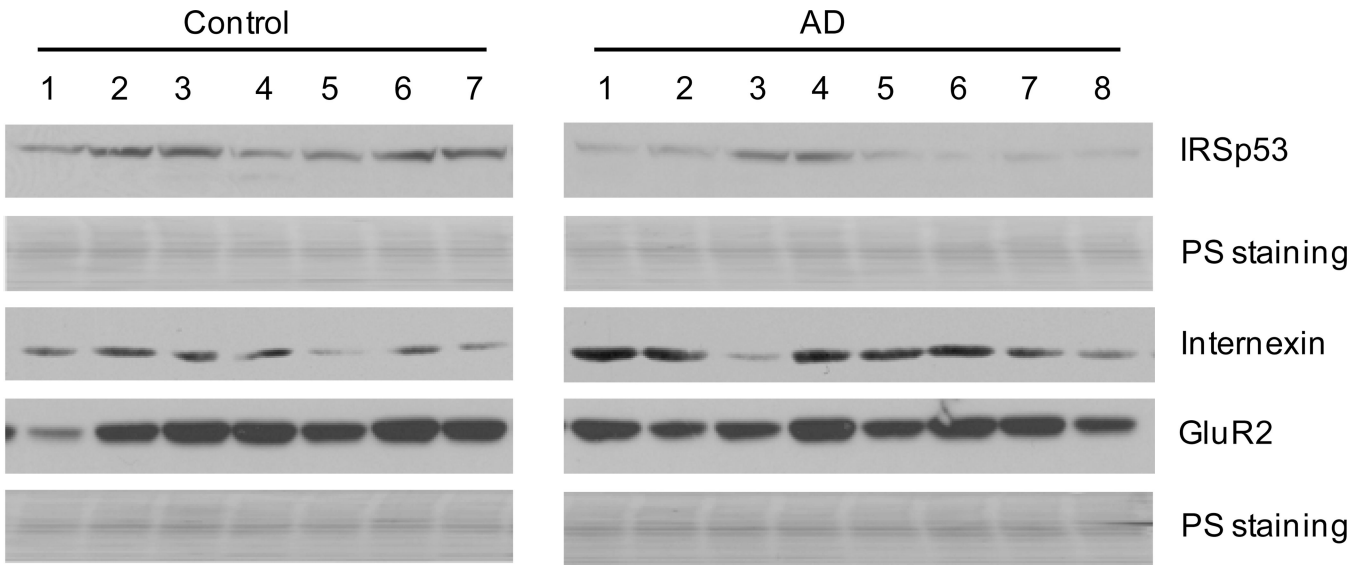

Figure 5. Immunoblot validation of AQUA discovered AD regulated PSD proteins

Individual post-mortem tissue samples from control and AD cases were probed for selected PSD associated proteins. Ponceau S staining (PS) shows the overall proteomic profile of each clinical specimen.

Clin Chim Acta. Author manuscript; available in PMC 2014 May 01.

Table 1

Proteins with altered levels in isolated PSD (AD versus control cases)

Accession#	Protein names	Data from two groups (log2 ratios)				Averaged log2 ratios to Ctl		
		pAD1/Ctl1	AD1/Ctl1	pAD2/Ctl2	AD2/Ctl2	Ctl/Ctl	pAD/Ctl	AD/Ctl
Cell adhesion								
NP_003079.1	fascin 1	0.44	0.92	−0.21	2.7	0	0.12	1.81
NP_116116.1	internexin neuronal intermediate filament	0.49	0.91	1.63	1.75	0	1.06	1.33
NP_000524.3	proteolipid protein 1	−0.01	−1.22	−1.32	−1.05	0	−0.67	−1.14
Chaperones								
NP_006576.2	chaperonin containing TCP1, subunit 8 (theta)	1.45	5.02	2.81	2.12	0	2.13	3.57
Cytoskeleton								
NP_005373.1	neurofilament 3 (150kDa medium)	1.1	1.3	1.05	1.7	0	1.08	1.50
NP_003118.1	spectrin, alpha, non-erythrocytic 1 (alpha-fodrin)	−0.03	0.84	1.52	0.92	0	0.75	0.88
NP_003119.1	spectrin, beta, non-erythrocytic 1	0.19	1.23	1.15	1.24	0	0.67	1.24
Metabolism								
NP_000166.2	glucose phosphate isomerase	−0.27	2.77	0.77	3.79	0	0.25	3.28
NP_000427.1	3-oxoacid CoA transferase 1 precursor	−0.75	1.18	2.29	3.9	0	0.77	2.54
NP_006614.2	phosphoglycerate dehydrogenase	0.51	0.83	2.01	3.34	0	1.26	2.09
NP_002620.1	phosphoglycerate mutase 1 (brain)	−0.02	2.02	1.11	1.78	0	0.55	1.90
Mitochondria								
NP_001853.2	cytochrome c oxidase subunit Vb precursor	−0.04	−1.22	−1.7	−3.42	0	−0.87	−2.32
NP_004640.1	es1 protein isoform Ia precursor	0.07	1.02	2.47	2.12	0	1.27	1.57
NP_006830.1	inner membrane protein, mitochondrial	−0.47	−0.99	−0.85	−2.44	0	−0.66	−1.72
NP_055157.1	mitochondrial carrier homolog 2	−0.34	−1.06	−0.99	−2.39	0	−0.67	−1.73
NP_004539.1	NADH dehydrogenase (ubiquinone) 1 beta	−0.18	−1.07	−0.95	−2.6	0	−0.57	−1.84
NP_066552.1	NADH dehydrogenase (ubiquinone) flavoprotein 2	0	−0.87	−0.81	−1.9	0	−0.41	−1.39

Accession#	Protein names	Data from two groups (log2 ratios)				Averaged log2 ratios to Ctl		
		pAD1/Ctl1	AD1/Ctl1	pAD2/Ctl2	AD2/Ctl2	Ctl/Ctl	pAD/Ctl	AD/Ctl
Signal transduction								
NP_005726.1	ARP1 actin-related protein 1 homolog B	−0.17	1.31	1.05	1.55	0	0.44	1.43
NP_006391.1	dynactin 2	0.08	0.85	0.89	1.26	0	0.49	1.06
NP_004263.1	homer 1	0.19	0.84	0.93	1.27	0	0.56	1.06
NP_006784.1	peroxiredoxin 3	−0.05	1.83	0.34	1.45	0	0.15	1.64
NP_006308.3	brain abundant, membrane attached signal protein 1	−1.15	−1.71	−2.67	−2.19	0	−1.91	−1.95
NP_057215.2	ras-related GTP-binding protein RAB10	−0.31	−1.18	−0.68	−1.61	0	−0.50	−1.40
NP_941959.1	Ras-related protein Rab-15	−0.43	−1.08	−0.63	−1.31	0	−0.53	−1.20
NP_003376.2	visinin-like 1	−0.39	−1.4	−1.31	−1.41	0	−0.85	−1.41